J Mol Model (2006) 12: 703–711
DOI 10.1007/s00894-005-0047-1

ORIGINAL PAPER

William N. Setzer · Glenn F. Rozmus · Mary C. Setzer · Jennifer M. Schmidt · Bernhard Vogler · Sabine Reeb · Betsy R. Jackes · Anthony K. Irvine

Bioactive principles in the bark of *Pilidiostigma tropicum*

Received: 13 May 2005 / Accepted: 27 September 2005 / Published online: 7 April 2006

Abstract The crude dichloromethane bark extract of *Pilidiostigma tropicum* (Myrtaceae) from north Queensland, Australia, shows antibacterial and cytotoxic activity. Bioactivity-directed separation led to the isolation of rhodomyrtoxin B and ursolic acid-3-*p*-coumarate as the biologically active materials. The structures of these compounds were elucidated on the basis of spectral analysis. The intercalation interaction of rhodomyrtoxin B with DNA was investigated using molecular mechanics and ab initio molecular-orbital techniques. A favorable π–π interaction between rhodomyrtoxin B and the cytosine–guanine base pair is predicted, but the orientation of the interaction cannot be predicted based on frontier molecular orbitals.

Keywords Cytotoxicity · Antibacterial · *Pilidiostigma tropicum* · Rhodomyrtoxin B · Ursolic acid coumarate · Intercalation

Dedicated to Professor Dr. Paul von Ragué Schleyer on the occasion of his 75th birthday

W. N. Setzer (✉) · G. F. Rozmus · M. C. Setzer · J. M. Schmidt · B. Vogler
Department of Chemistry, University of Alabama in Huntsville, Huntsville, AL 35899, USA
e-mail: wsetzer@chemistry.uah.edu
Tel.: +1-256-8246519
Fax: +1-256-8246349

S. Reeb
Institut für Chemie, Universität Hohenheim, 70599 Stuttgart, Germany

B. R. Jackes
School of Tropical Biology, James Cook University, Townsville Queensland 4811, Australia

A. K. Irvine
C. S. I. R. O., Tropical Forest Research Centre, Atherton Queensland 4883, Australia

Introduction

The Myrtaceae is a significant family in herbal medicine throughout the world. Important Australian members of the family include *Eucalyptus globulus* ("blue gum") and *Melaleuca alternifolia* ("tea tree") [1]. We have been interested in Australian tropical rainforest members of the family, [2] and in this work we have examined *Pilidiostigma tropicum* L.S. Smith (common name: Apricot Myrtle) from north Queensland, Australia. To our knowledge, there are no references to any ethnobotanical uses of this tree, nor have there been any previously reported phytochemical or pharmacological investigations.

P. tropicum is endemic to the Wet Tropics region of north Queensland, Australia, between the Paluma Range and just south of Cooktown [3]. Within this region it is a widespread understory tree, up to 18 m. tall, with opposite, simple leaves and flaky, often fissured bark. Its altitudinal range is from near sea level to 1,000 m. and it occurs on a wide range of soil types.

In this paper, we present the isolation and biological activities of the cytotoxic and antibacterial principles from *P. tropicum*. We also present a theoretical investigation of the π–π interactions between rhodomyrtoxin B and the guanine–cytosine base pair in order to determine if the lowest-energy orientations of intercalation can be predicted based upon frontier molecular orbital interactions.

Materials and methods

Collection and extraction of plant material

Bark samples from several specimens of *P. tropicum* were collected 6th August, 1997, from a complex notophyll vine forest [4] at ca. 720 m a.s.l. at the Curtain Fig State Forest, Australia (17°17' S, 145°34' E) under permit issued to A. K. Irvine (C.S.I.R.O.). Voucher specimens have been

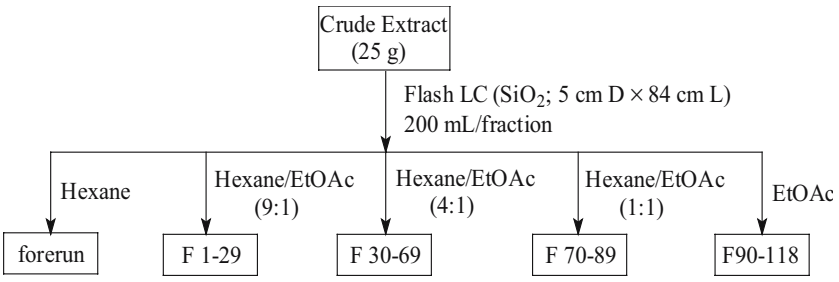

Scheme 1 Separation of *Pilidiostigma tropicum* crude bark extract by flash liquid chromatography

deposited with the C.S.I.R.O. (A.K. Irvine 1707) and the James Cook University Herbaria. The stem bark (988 g) was chopped and extracted with a 1:1 mixture of chloroform/ethanol (24 h) to give 45.8 g extract.

Biological screening

The crude bark extract, chromatographic fractions, and purified compounds were screened for antimicrobial activity against Gram-positive bacteria, *Bacillus cereus* (ATCC No. 14579) and *Staphylococcus aureus* (ATCC No. 29213), and Gram-negative bacteria, *Pseudomonas aeruginosa* (ATCC No. 27853) and *Escherichia coli* (ATCC No. 25922) as previously described [2]. The materials were screened for cytotoxic activity against Human Hep G2 hepatocellular carcinoma cells (ATCC No. HB-8065) [5] and Human MDA-MB-231 mammary adenocarcinoma cells (ATCC No. HTB-26) [6] as described previously [2].

Bioactivity-directed isolation

The crude bark extract (25.0 g) was subjected to bioactivity-directed flash chromatography (Scheme 1); on a silica gel (230–400 mesh) column (84 cm L×5 cm D). Elution was carried out using a hexane/ethyl acetate step gradient (hexane, 9:1 hexane/EtOAc, 4:1 hexane/EtOAc, 1:1 hexane/EtOAc, EtOAc) with detection of eluates by TLC. Bioactivity screening of fractions led to two biologically active compounds: rhodomyrtoxin B (recrystallized from F32-33 to give 867 mg) [7] and ursolic acid-3-*p*-coumarate (recrystallized from F77 to give 86.7 mg). [8] Structures were determined by comparison of ^{1}H and ^{13}C NMR and MS with those reported in the literature. The biological activities of these materials are presented in Table 1.

Computational studies

Hartree-Fock *ab initio* calculations at the 3-21G(*) level were carried out using both GAUSSIAN 98W and SPARTAN '04 computer programs. The π–π interaction of rhodomyrtoxin B with the cytosine–guanine (C–G) base pair was investigated at the post-Hartree-Fock level, using the MP2/6-31G* method, as implemented by the GAUSSIAN 98W computer program. The structures of rhodomyrtoxin B and the base pair (assuming planarity) were optimized at the HF 3-21G(*) level. Single-point MP2/6-31G* calculations were carried out using different coplanar orientations and positions of rhodomyrtoxin B, held at 3.4 Å above the plane of the base pair, to map the energy surface. Molecular mechanics calculations using MM2 were carried out to investigate the intercalation of rhodomyrtoxin B with a C-G dimer, 3.4 Å separation, using the preferred orientation of rhodomyrtoxin B with C-G.

Results

The crude bark extract of *P. tropicum* showed *in vitro* cytotoxic activity against Hep-G2 (human hepatocellular carcinoma) and MDA-MB-231 (human mammary adenocarcinoma) cell lines, as well as antibacterial activity against the Gram-positive bacteria *Bacillus cereus* and *Staphylococcus aureus* (Table 1). Bioactivity-directed flash chromatographic separation (Scheme 1) led to two biologically active compounds: rhodomyrtoxin B and

Table 1 Cytotoxic and antibacterial activities of *Pilidiostigma tropicum* bark extract and constituents

Material	Cytotoxicity (LC_{50})		Antibacterial activity (MIC)	
	Hep-G2	MDA-MB-231	*Bacilluscereus*	*Staphylococcus aureus*
P. tropicum crude bark extract	95.6±0.7% kill at 250 μg/ml	100% kill at 250 μg/ml	<19.5 μg/ml	<19.5 μg/ml
Rhodomyrtoxin B	19.0(±9.0) μM	2.50(±0.27) μM	0.14 μM	0.28 μM
Ursolic acid-3-*p*-coumarate	1.43(±0.36) μM	15.3(±3.1) μM	1.63 μM	6.5 μM
Positive control	1.19(±0.67) μM[a]	9.23(±7.89) μM[a]	2.14 μM[b]	1.07 μM[b]

[a]Vinblastine sulfate
[b]Gentamicin sulfate

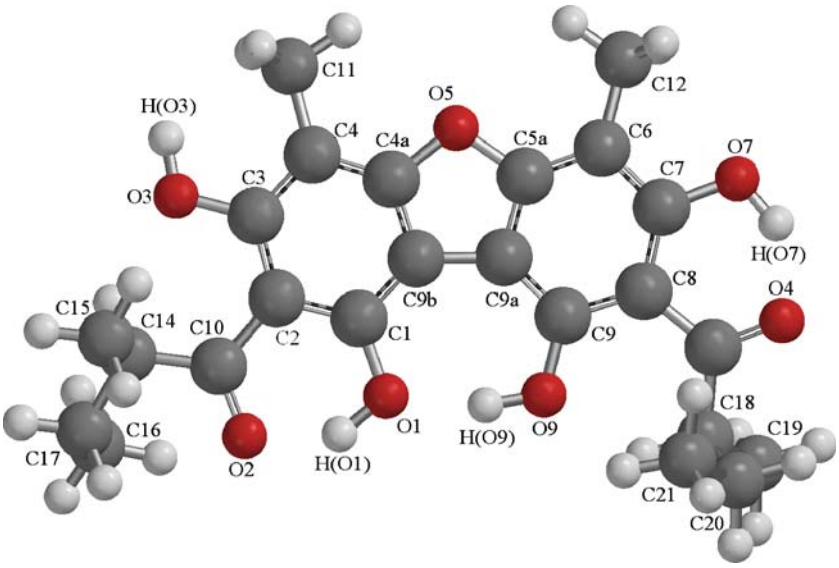

Fig. 1 HF 3-21G(*) optimized structure and numbering scheme of rhodomyrtoxin B

ursolic acid-3-*p*-coumarate. The biological activities of these materials are presented in Table 1.

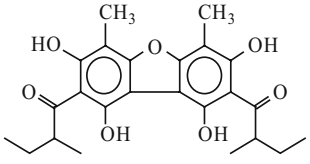

Rhodomyrtoxin B

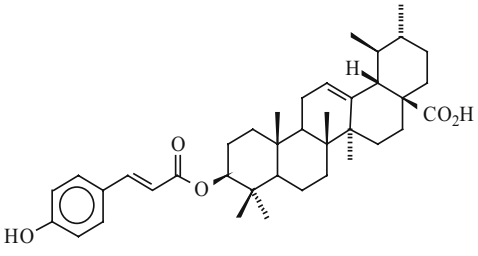

Ursolic acid-3-*p*-coumarate

The 3-21G(*) optimized structures for rhodomyrtoxin B, and the cytosine–guanine base pair are shown in Figs. 1 and 2, respectively. Mulliken atomic charges, HF 3-21G (*), for rhodomyrtoxin B, cytosine, and guanine are listed in Tables 2 and 3. Frontier–molecular–orbital (FMO) energies for C–G are: HOMO=−7.35 eV, LUMO=2.39 eV; and for rhodomyrtoxin B are: HOMO=−7.69 eV, LUMO=1.89 eV. Thus, the important frontier–molecular–orbital interactions are expected to be the HOMO of cytosine–guanine and the LUMO of rhodomyrtoxin B. These FMO's are shown in Fig. 3. Mapping the π–π interaction energy between rhodomyrtoxin B and the C-G base pair at the MP2/6-31G* level revealed six low-energy orientations (Figs. 4, 5, 6, 7, 8 and 9). Molecular mechanics (MM2) calculations indicate that the lowest-energy orientation from the ab initio study cannot be accommodated in an intercalative model. Thus, the MM2 strain energy increase in intercalation of rhodomyrtoxin B into the C–G complementary dimer is 82.7 kcal mol^{-1} (see Fig. 10).

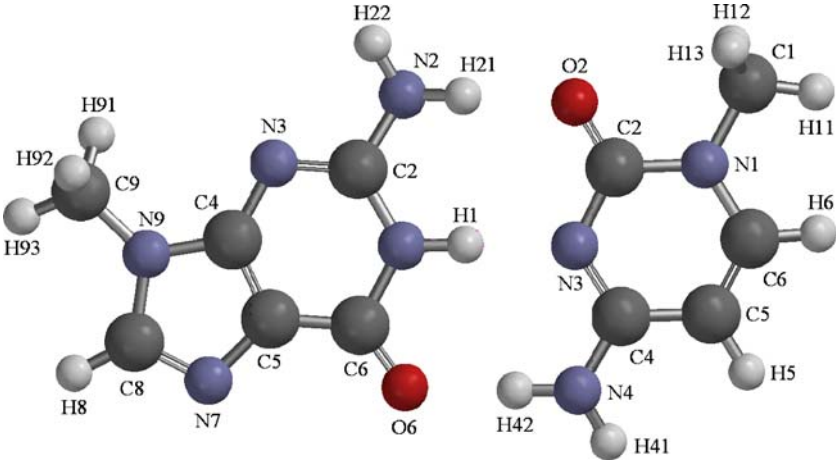

Fig. 2 HF 3-21G(*) optimized structure (constrained to be planar) and numbering scheme of guanine–cytosine

Table 2 Mulliken atomic charges, HF 3-21G(*), of rhodomyrtoxin B

Atom	Charge	Atom	Charge
C1	0.498	O3	−0.760
C2	−0.267	H(O3)	0.426
C3	0.431	C11	−0.616
C4	−0.135	Ha(C11)	0.275
C4a	0.445	Hb(C11)	0.221
O5	−0.768	Hc(C11)	0.220
C5a	0.425	C12	−0.544
C6	−0.153	Ha(C12)	0.233
C7	0.517	Hb(C12)	0.232
C8	−0.296	Hc(C12)	0.215
C9	0.460	O7	−0.790
C9a	−0.077	H(O7)	0.458
C9b	−0.064	C13	0.732
O1	−0.847	O4	−0.681
H(O1)	0.481	C18	−0.433
C10	0.731	H(C18)	0.297
O2	−0.680	C19	−0.548
C14	−0.415	Ha(C19)	0.228
H(C14)	0.278	Hb(C19)	0.200
C15	−0.556	Hc(C19)	0.199
Ha(C15)	0.221	C20	−0.380
Hb(C15)	0.214	Ha(C20)	0.226
Hc(C15	0.212	Hb(C20)	0.208
C16	−0.379	C21	−0.600
Ha(C16)	0.236	Ha(C21)	0.218
Hb(C16)	0.206	Hb(C21)	0.202
C17	−0.593	Hc(C21)	0.197
Ha(C17)	0.213		

Table 3 Mulliken atomic charges, HF 3-21G(*), of cytosine and guanine

Guanine		Cytosine	
Atom	Charge	Atom	Charge
N1	−1.048	N1	−0.943
H1	0.477	C1	−0.327
C2	1.020	H11	0.209
N2	−0.915	H12	0.248
H21	0.399	H13	0.249
H22	0.346	C2	1.141
N3	−0.813	O2	−0.674
C4	0.772	N3	−0.885
C5	0.028	C4	0.814
C6	0.946	N4	−0.940
O6	−0.696	H41	0.342
N7	−0.629	H42	0.440
C8	0.344	C5	−0.423
H8	0.266	H5	0.259
N9	−0.933	C6	0.266
C9	−0.321	H6	0.291
H91	0.249		
H92	0.225		
H93	0.216		

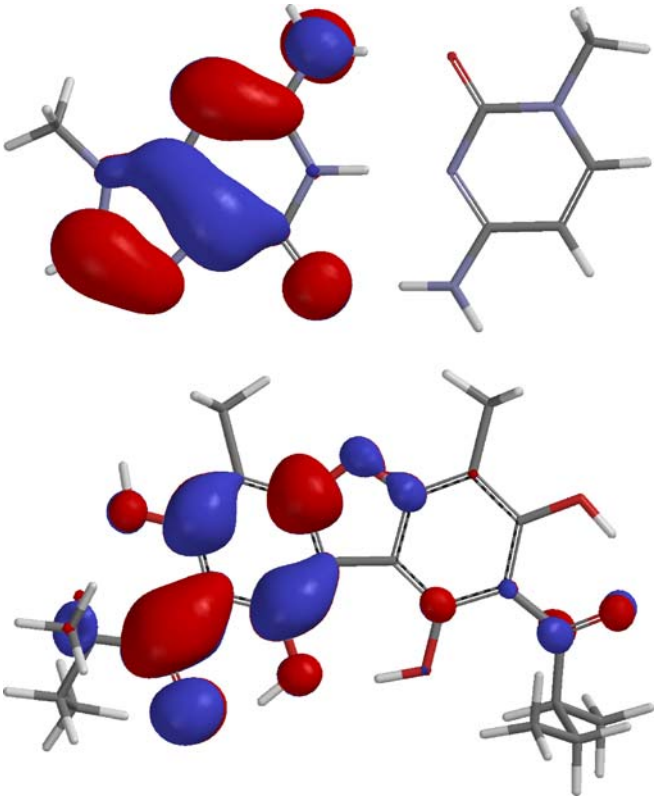

Fig. 3 HOMO of C–G and LUMO of rhodomyrtoxin B

Discussion

Rhodomyrtoxin B, isolated previously from *Rhodomyrtus macrocarpa*, [7] is a dibenzofuran derivative. This class of compounds has exhibited remarkable bioactivity, most notably the polychlorinated dibenzofurans, [9] but natural dibenzofurans are active as well [10–14]. Dibenzofurans are known to bind to the aryl hydrocarbon receptor [15] as well as to intercalate into DNA [16–20].

Ursolic acid [21] as well as coumarate esters of terpenoids have also shown cytotoxic activity [22–24]. Ursolic acid itself has been shown to inhibit the enzymes

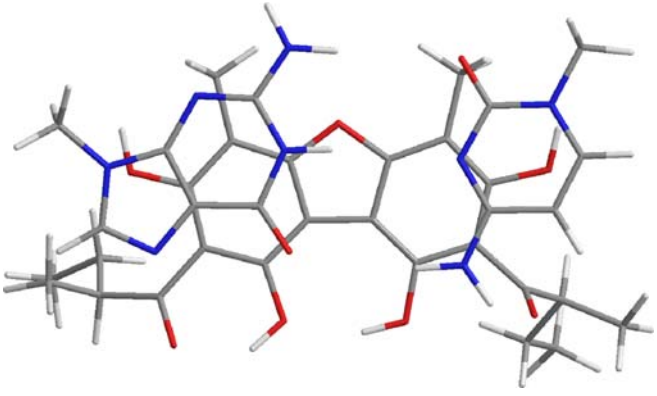

Fig. 4 Lowest-energy orientation of rhodomyrtoxin B with cytosine–guanine

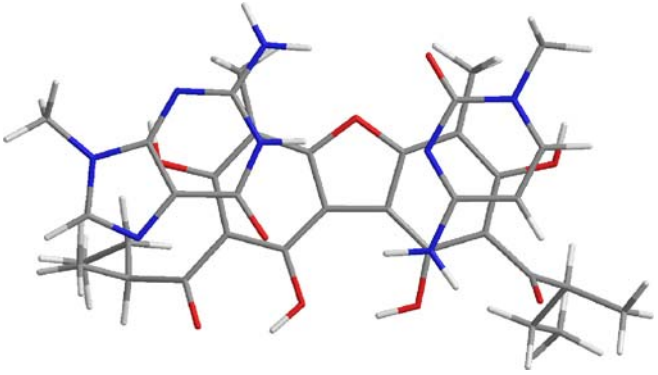

Fig. 5 Low-energy (E_{rel}=1.47 kcal mol^{-1}) orientation of rhodomyrtoxin B with cytosine–guanine

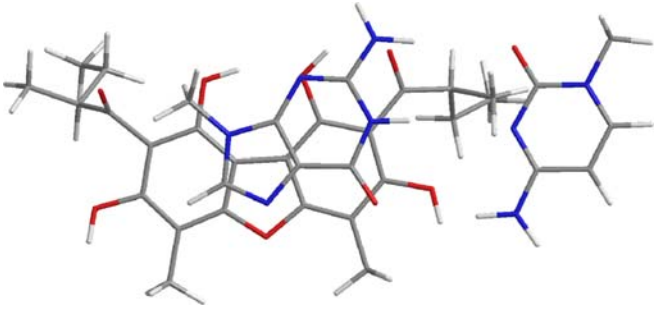

Fig. 7 Low-energy (E_{rel}=2.20 kcal mol^{-1}) orientation of rhodomyrtoxin B with cytosine–guanine

topoisomerase I and II, DNA polymerase, lipoxygenase, and tyrosine kinase, and induces apoptosis possibly involving activation of caspases [25]. Hydroxycinnamic esters probably exhibit their bioactivity by inhibition of respiratory chain-linked electron transport. The lipophilic triterpenoid allows penetration into membranes and the phenolic moiety produces stable free radicals, thus interfering with redox reactions [26, 27].

Interactions between π-systems such as benzene dimer [28, 29], naphthalene dimer [30], substituted benzenes with benzene [31, 32], substituted benzenes with aromatic nitrogen bases, [33] and guanine assemblies, [34] have been studied computationally as model systems for π–π interactions [35]. Dispersion interactions, which have their origins in electron correlation, are important facets in π–π interactions, and therefore, electron correlation must be included [36, 37]. In this study, the second order Møller–Plesset perturbation (MP2) [38] was used to account for correlation effects.

Intercalating antitumor drugs [39] function by forming a ternary cleavable complex with DNA and various DNA polymerases. These drugs intercalate or otherwise insert themselves into DNA and form a complex with proteins such as topoisomerase I and II that replicate and repair DNA such that they cannot continue to move along the DNA strand [40–43]. These agents have the greatest effect on cells that replicate rapidly and/or frequently, as tumor cells are known to do [40, 44]. DNA-intercalating ligands are a diverse group of compounds containing an aromatic chromophore that bind reversibly to double-stranded DNA by insertion between base pairs [45, 46]. Drugs that are currently used to treat cancers and leukemias such as doxorubicin and amsacrine [47] have been shown to intercalate into the DNA of these rapidly proliferating cells. Intercalating agents like these are typically aromatic heterocycles comprised of three fused six-membered rings. It is not known whether these agents exhibit sequence selectivity beyond two or three base pairs.

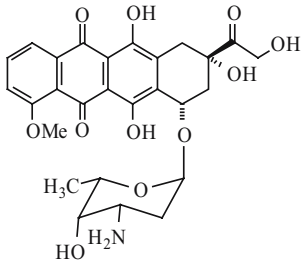

Doxorubicin

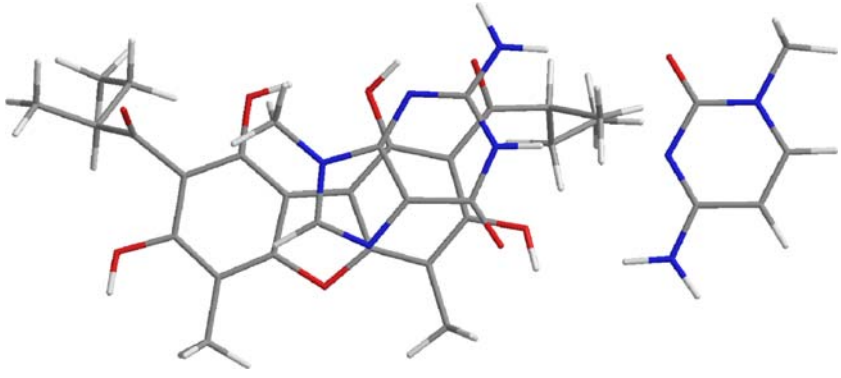

Fig. 6 Low-energy (E_{rel}= 1.95 kcal mol^{-1}) orientation of rhodomyrtoxin B with cytosine–guanine

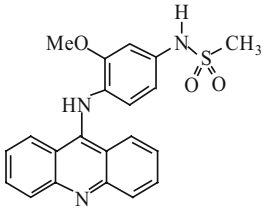

Amsacrine

Experimental structural studies of intercalating ligands and oligonucleotides have been carried out in the solid state using X-ray crystallography [48, 49] and in solution using high-resolution NMR techniques [50–56]. Interaction of DNA intercalators has been modeled using molecular mechanics/molecular dynamics [47, 57–61]. These modeling studies have concentrated on electrostatic interactions and hydrogen bonding. Although it is commonly accepted [47] that intercalating ligands align themselves within the DNA helix to "effect optimal π overlap with the two base pairs that constitute the binding site, there is no theory available that adequately explains the nature of the hydrophobic forces in nucleic acids" [62]. Nucleotide base stacking has been examined using high-level ab initio methods [63–65]. These workers have concluded that electron correlated ab initio calculations are strictly required for obtaining reliable energies for π–π interactions, and that density functional (DFT) methods fail to adequately describe nucleotide stacked base pairs. Recently, Reha and co-workers [66] have examined the nature of intercalative interactions of ethidium, daunomycin, ellipticine, and 4',6-diaminide-2-phenylindole with DNA base pairs using ab initio, density functional theory (DFT), and empirical potential methods. These workers have concluded that only theoretical procedures properly covering dispersion, polarization, and charge-transfer effects can be used to study intercalation. Thus, simple Hartree-Fock (HF) methods or DFT/B3LYP methods are not recommended; whereas inclusion of Møller-Plesset second order electron correlation (MP2) or DFTB-D methods provide the dispersion energy necessary for π–π stacking.

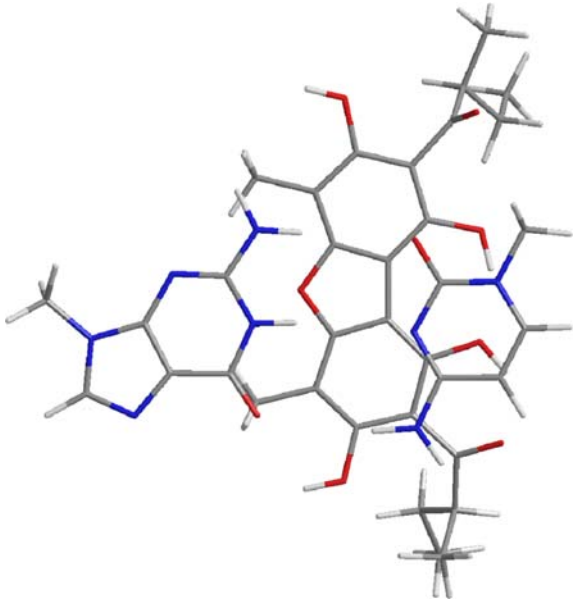

Fig. 8 Low-energy (E_{rel}=2.53 kcal mol^{-1}) orientation of rhodomyrtoxin B with cytosine–guanine

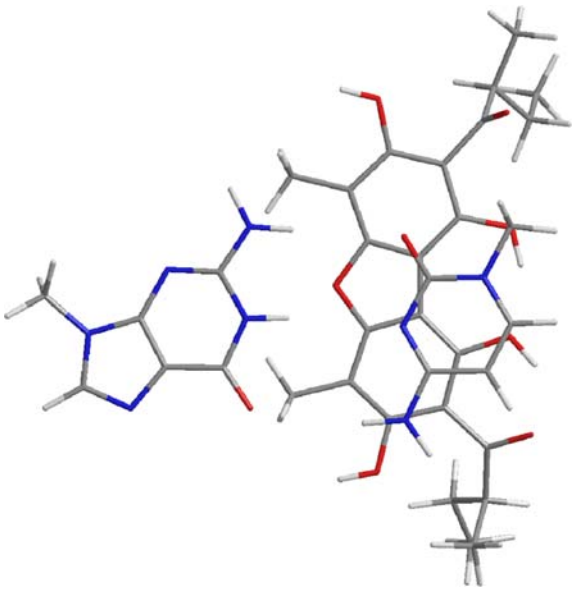

Fig. 9 Low-energy (E_{rel}=2.59 kcal mol^{-1}) orientation of rhodomyrtoxin B with cytosine–guanine

Frontier–molecular–orbital interactions have been considered in π-stacking (self organization) of naphthalene with pyromellitimide [67]. The self-organized π-stacked naphthalene-pyromellitimide-naphthalene sandwich shows favorable orbital overlap between the highest occupied molecular orbital (HOMO) of naphthalene and the lowest unoccupied molecular orbital (LUMO) of pyromellitimide. In the case of rhodomyrtoxin B and the C–G base pair, the HOMO of the base pair is located on guanine while the LUMO of rhodomyrtoxin B is located predominantly on one of the benzene rings (see Fig. 3). However, the lowest energy orientation of rhodomyrtoxin B with the C–G base pair (Fig. 4) does not allow maximum complementary overlap of the HOMO of C–G with the LUMO of rhodomyrtoxin B. Indeed, the orientation that gives the best frontier molecular orbital overlap pictorially is 13.5 kcal mol^{-1} higher in energy than the lowest-energy orientation. Thus, in this case, favorable frontier–molecular–orbital overlap cannot be used to predict the preferred orientation of the intercalator.

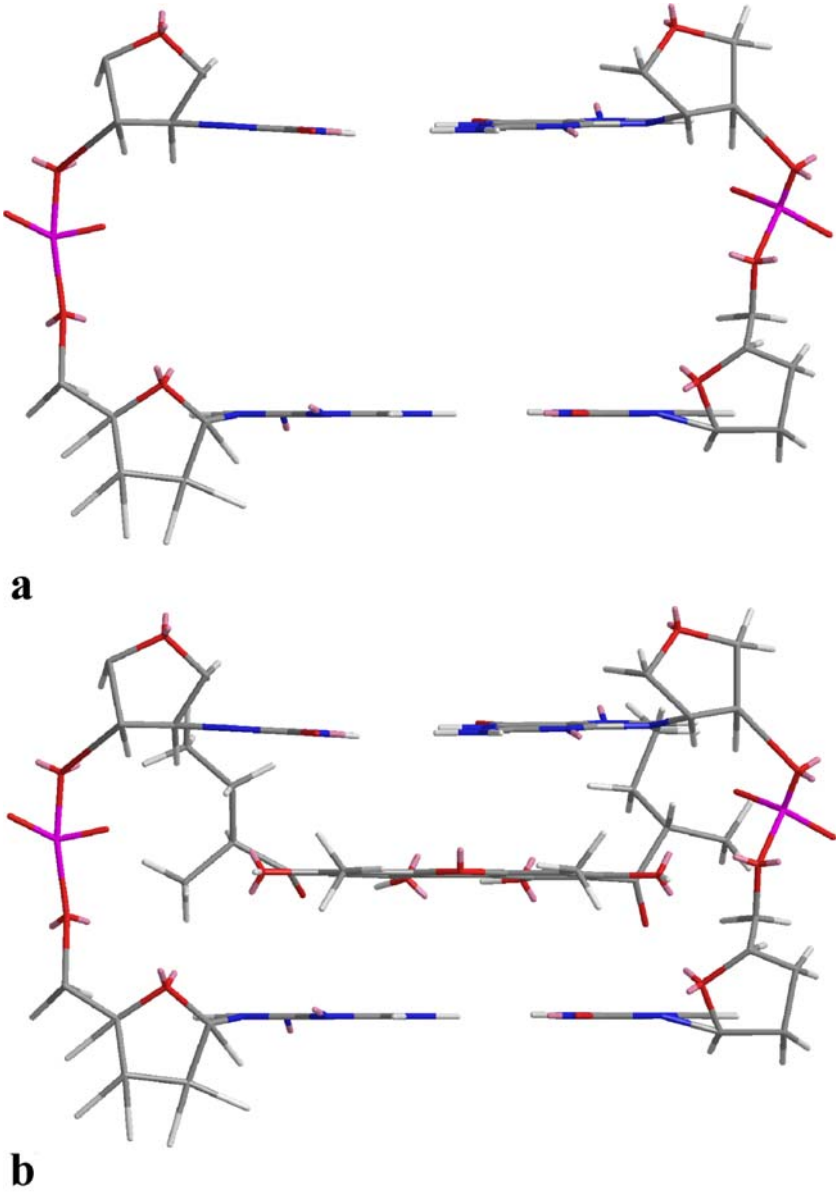

Fig. 10 Intercalation model of rhodomyrtoxin B with a C–G duplex (**a** base-pair separation of 6.8 Å. **b** intercalation of rhodomyrtoxin B)

Electrostatic interactions are generally considered to be important for DNA intercalation. Thus, for example, electrostatic interactions play a major role in the positioning of 9-aminoacridine as a DNA intercalator and a significant stabilizing role in the binding of ethidium in DNA [68]. Examination of the atomic charges on rhodomyrtoxin B and the C–G base pair does not reveal compelling evidence of favorable electrostatic interactions in this case, however. Dipole–dipole interactions may also be important in DNA intercalation. It has been suggested that intercalation of methylene blue between DNA base pairs is stabilized by favorable dipole-dipole interactions as well as π–π interactions [69]. The molecular dipoles of rhodomyrtoxin B and the C–G base pair in the lowest-energy orientation do, in fact, align in nearly opposite directions (Fig. 11). Thus, dipole–dipole interactions may be the important interaction governing the orientation of rhodomyrtoxin B in DNA.

Conclusions

The bioactive agents responsible for the cytotoxic and antimicrobial activity of the crude bark extract of *Pilidiostigma tropicum* are rhodomyrtoxin B and ursolic acid-3-*p*-coumarate. These compounds exhibit bioactivities comparable to the antitumor drug vinblastine or the antibiotic gentamicin. The computational results from this study are consistent with an intercalative mechanism as the possible source of the cytotoxic activity of rhodomyrtoxin B. Although lowest-energy positions and orientations of rhodomyrtoxin B with the C–G base pair have been

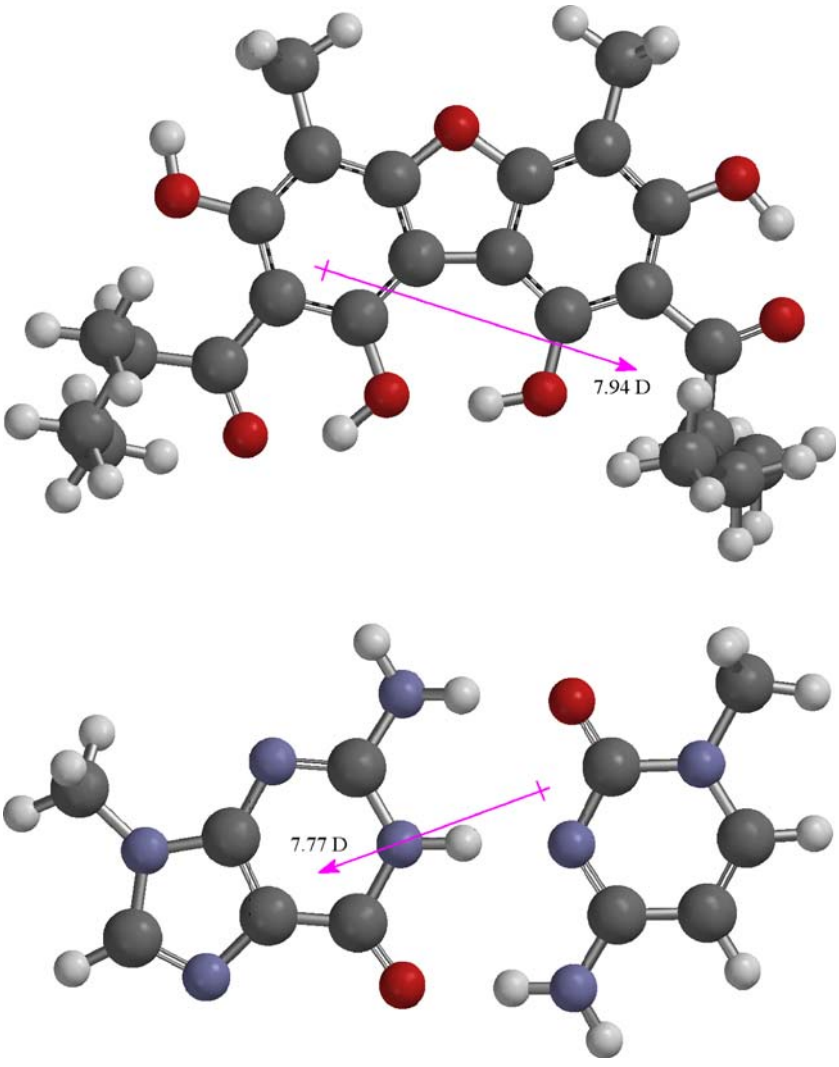

Fig. 11 Calculated molecular dipoles of rhodomyrtoxin B and C–G base pair

calculated using the MP2 method, these positions cannot be predicted based upon simple frontier-molecular–orbital interactions, electrostatic interactions, or dipole-dipole interactions. Steric interactions of the alkyl side chains of rhodomyrtoxin B may also preclude these orientations in DNA itself.

Acknowledgements Support for this research was provided in part by a grant from the National Institutes of Health (Grant No. 1 R15 AIOD39740-01). We are grateful to the Queensland Forest Service for allowing us access to the Curtain Fig State Forest. We thank Ms. Susan M. Fields for assistance with the cytotoxicity screening.

References

1. Lassak EV, McCarthy T (1990) Australian medicinal plants. Mandarin Press, Melbourne, Australia
2. Setzer MC, Setzer WN, Jackes BR, Gentry GA, Moriarity DM (2001) Pharmaceut Biol 39:67–78
3. Hyland BPM, Whiffen T (1993) Australian tropical rain forest trees, vol 2. C.S.I.R.O., Melbourne, Australia
4. Tracey JG (1982) The vegetation of the humid tropical region of North Queensland. C.S.I.R.O., Melbourne, Australia
5. Knowles BB, Howe CC, Aden DP (1980) Science 209: 497–499
6. Cailleau R, Young R, Olive M, Reeves WJ (1974) J Natl Cancer Inst 53:661–674
7. Igboechi CA, Parfitt RT, Rowan MG (1984) Phytochemistry 23:1139–1141
8. Yasue M, Sakakibara J, Ina H (1973) Yakugaku Zasshi 93: 687–691
9. Safe SH (1994) Crit Rev Toxicol 24:87–149
10. Carney JR, Scheuer PJ (1993) Tetrahedron Lett 34:3727–3730
11. Kokubun T, Harborne JB, Eagles J, Waterman PG (1995) Phytochemistry 38:57–60
12. Kokubun T, Harborne JB, Eagles J, Waterman PG (1995) Phytochemistry 39:1039–1042
13. Kumar KC, Muller K (1999) J Nat Prod 62:821–823
14. Ingolfsdottir K (2002) Phytochemistry 61:729–736
15. Hahn ME (1998) Comp Biochem Physiol C 121:23–53
16. Wang S, Hall JE, Tanious FA, Wilson WD, Patrick DA, McCurdy DR, Bender BC, Tidwell RR (1999) Eur J Med Chem 34:215–224
17. Yamada M, Kato K, Shindo K, Nomizu M, Haruki M, Sakairi N, Ohkawa K, Yamamoto H, Nishi N (2001) Biomaterials 22:3121–3126

18. Yamada M, Kato K, Nomizu M, Ohkawa K, Yamamoto H, Nishi N (2002) Environ Sci Technol 36:949–954
19. Zhao C, Liu X, Nomizu M, Nishi N (2004) J Coll Interface Sci 275:470–476
20. Liu XD, Murayama Y, Matsunaga M, Nomizu M, Nishi N (2005) Int J Biol Macromol 35:193–199
21. Lee KH, Lin YM, Wu TS, Zhang DC, Yamagishi T, Hayashi T, Hall IH, Chang JJ, Wu RY, Yang TH (1988) Planta Med 54:308–311
22. Numata A, Yang P, Takahashi C, Fujiki R, Nabae M, Fujita E (1989) Chem Pharm Bull 37:648–651
23. Kashiwada Y, Zhang DC, Chen YP, Cheng CM, Chen HT, Chang HC, Chang JJ, Lee KH (1993) J Nat Prod 56:2077–2082
24. Setzer WN, Setzer MC, Bates RB, Nakkiew P, Jackes BR, Chen L, McFerrin MB, Meehan EJ (1999) Planta Med 65:747–749
25. Setzer WN, Setzer MC (2003) Mini Rev Med Chem 3:540–556
26. Kubo I, Fujita KI, Nihei KI, Masuoka N (2003) Bioorg Med Chem 11:573–580
27. Sakihama Y, Cohen MF, Grace SC, Yamasaki H (2002) Toxicology 177:67–80
28. Tsuzuki S, Honda K, Uchimaru T, Mikami M, Tanabe K (2002) J Am Chem Soc 124:104–112
29. Sinnokrot MO, Valeev EF, Sherrill CD (2002) J Am Chem Soc 124:10887–10893
30. Tsuzuki S, Uchimaru T, Matsumura K, Mikami M, Tanabe K (2000) Chem Phys Lett 319:547–554
31. Sinnokrot MO, Sherrill CD (2004) J Am Chem Soc 126: 2690–2697
32. Mignon P, Loverix S, Geerlings P (2005) Chem Phys Lett 401:40–46
33. Chandra PP, Jain A, Sapse AM (2004) J Mol Model 10:1–5
34. Di Felice R, Calzolari A, Molinari E, Garbesi A (2002) Phys Rev B 65:045104
35. Waters ML (2002) Curr Opin Chem Biol 6:736–741
36. Pickholz M, Stafström S (2001) Chem Phys 270:245–251
37. Pickholz M, dos Santos MC (2005) J Mol Struct Theochem 717:99–106
38. Møller C, Plesset MS (1934) Phys Rev 46:618–622
39. Berman HM, Young PR (1981) Annu Rev Biophys Bioeng 10:87–114
40. Vivas-Mejia PE, Cox O, Gonzalez FA (1998) Mol Cell Biochem 178:203–212
41. Baez A, Riou JF, Le Pecq JB, Riou G (1989) Mol Pharmacol 37:377–382
42. Chen H, Patel DJ (1995) J Mol Biol 246:164–179
43. Tabarrini O, Cecchetti V, Fravolini A, Nocentini G, Barzi A, Sabatini S, Miao H, Sissi C (1999) J Med Chem 42:2136–2144
44. Dassoneville L, Lansiaux A, Wattelet A (2000) Eur J Pharmacol 409:9–18
45. Denny WA (1989) Anti-Cancer Drug Design 4:241–263
46. Baguley BC (1991) Anti-Cancer Drug Design 6:1–35
47. Neidle S, Jenkins TC (1991) Meth Enzymol 203:433–458
48. Todd AK, Adams A, Thorpe JH, Denny WA, Wakelin LPG, Cardin CJ (1999) J Med Chem 42:536–540
49. Adams A, Guss JM, Collyer CA, Denny WA, Wakelin LPG (1999) Biochemistry 38:9221–9233
50. Bunkenborg J, Stidsen MM, Jacobsen JP (1999) Bioconjugate Chem 10:824–831
51. Bostock-Smith CE, Gimenez-Arnau E, Missailidis S, Laughton CA, Stevens MFG, Searle MS (1999) Biochemistry 38: 6723–6731
52. Bible KC, Bible RH, Kottke TJ, Svingen PA, Xu K, Pang YP, Hajdu E, Kaufmann SH (2000) Cancer Res 60:2419–2428
53. Li Z, Tamura PJ, Wilkinson AS, Harris CM, Harris TM, Stone MP (2001) Biochemistry 40:6743–6755
54. Favier A, Blackledge M, Simorre JP, Crouzy S, Dabouis V, Gueiffier A, Marion D, Debouzy JC (2001) Biochemistry 40:8717–8726
55. Brown K, Hingerty BE, Guenther EA, Krishnan VV, Broyde S, Turteltaub KW, Cosman M (2001) Proc Natl Acad Sci USA 98:8507–8512
56. Han X, Gao X (2001) Curr Med Chem 8:551–581
57. Hill GC, Wunz TP, MacKenzie NE, Gooley PR, Remers WA (1991) J Med Chem 34:2079–2088
58. Cardozo MG, Hopfinger AJ (1991) Mol Pharmacol 40: 1023–1028
59. van der Klein-de Gunst FJM, van Boom JH, Liskamp RMJ (1992) J Comput Aided Mol Des 6:33–46
60. de Pascual-Teresa B, Gallego J, Ortiz AR, Gago F (1996) J Med Chem 39:4810–4824
61. Fisher G, Pindur U (1999) Pharmazie 54:83–93
62. Voet D, Voet JG (1995) Biochemistry, 2nd edn. Wiley, New York, pp 848–872
63. Sponer J, Leszczynski J, Hobza P (1996) J Phys Chem 100:5590–5596
64. Hobza P, Sponer J (1999) Chem Rev 99:3247–3276
65. Elstner M, Hobza P, Frauenheim T, Suhai S, Kaxiras E (2001) J Chem Phys 114:5149–5155
66. Reha D, Kabelac M, Ryjacek F, Sponer J, Sponer JE, Elstner M, Suhai S, Hobza P (2002) J Am Chem Soc 124:3366–3376
67. Cooray AS, de Silva KMN (2004) J Mol Struct Theochem 678:223–231
68. Medhi C, Mitchell JBO, Price SL, Tabor AB (1999) Biopolymers 52:84–93
69. Zhang LZ, Tang GQ (2004) J Photochem Photobiol B 74: 119–125